Electronic Supplementary Material (ESI) for Nanoscale.

Supplementary Information for

Alloying-assisted Phonon Engineering of Layered $BiInSe_3$@Nickel Foam for Efficient Solar-enabled Water Evaporation

J. D. Yao, Z. Q. Zheng and G. W. Yang*

State Key Laboratory of Optoelectronic Materials and Technologies, Nanotechnology Research Center, School of Materials Science & Engineering, School of Physics, Sun Yat-sen University, Guangzhou 510275, Guangdong, P. R. China.

*Corresponding author: stsygw@mail.sysu.edu.cn

S1. Experimental setup of the PLD system.

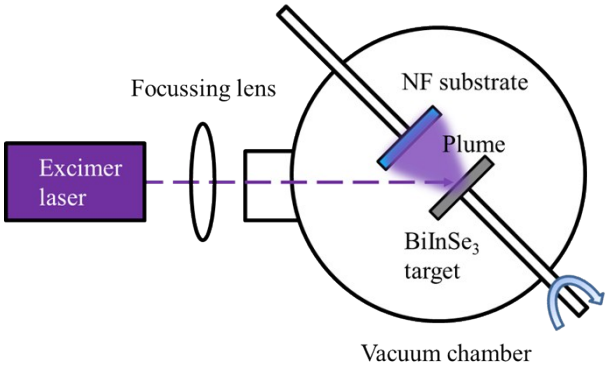

Fig. S1. Experimental setup of the PLD system.

S2. AFM thickness profile of the PLD-grown $BiInSe_3$.

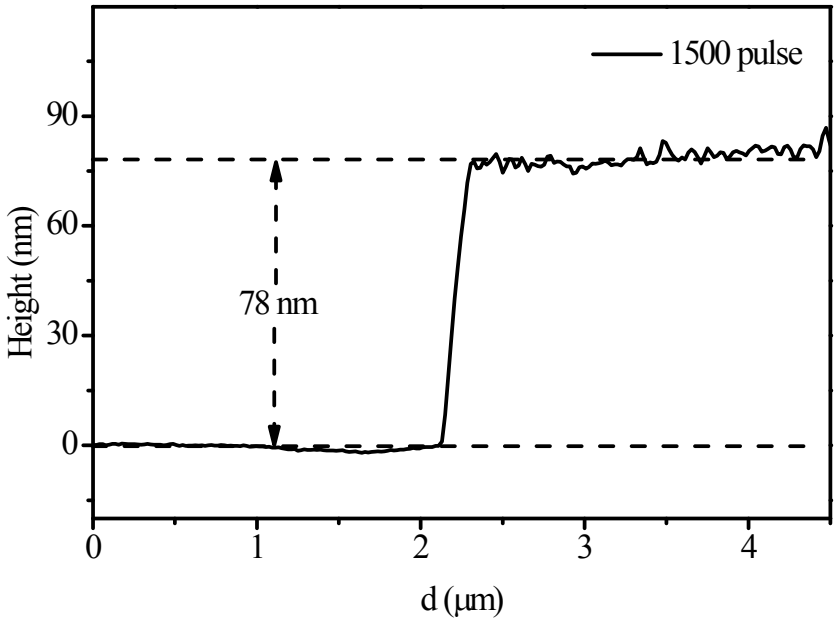

Fig. S2. AFM thickness profile of the PLD-grown $BiInSe_3$ film with a laser pulse number of 1500.

S3. Digital photograph and SEM image of pure NF.

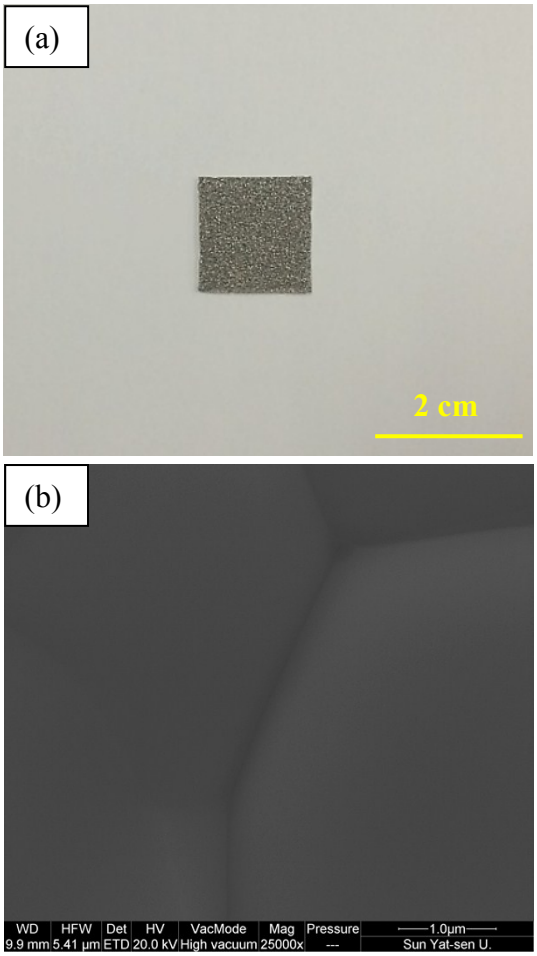

Fig. S3. (a) Digital photograph of pure NF. Scale bar: 2 cm. (b) High-magnification SEM image. Scale bar: 1 μm.

S4. Full spectrum XPS scan of the PLD-grown $BiInSe_3$.

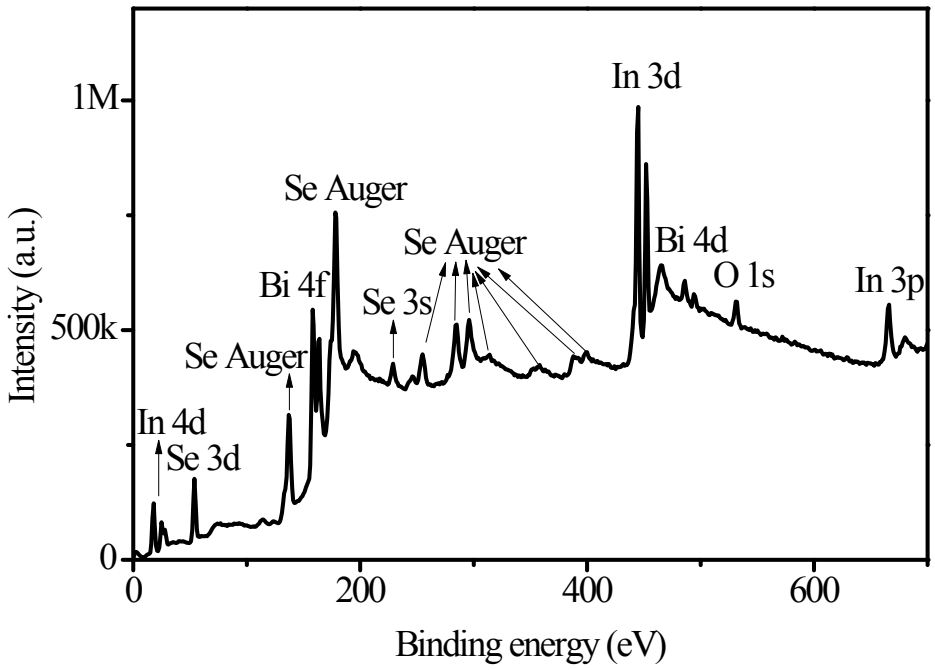

Fig. S4. Full spectrum XPS scan of the PLD-grown $BiInSe_3$.

S5. Reflectance spectrum of pure NF and $BiInSe_3$@NF in the solar spectrum range.

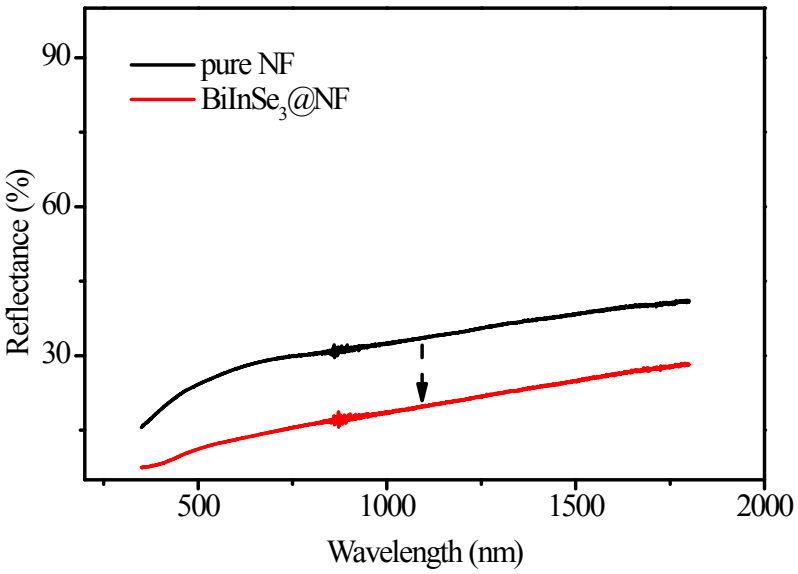

Fig. S5. Reflectance spectrum of pure NF and $BiInSe_3$@NF in the solar spectrum range.

S6. Photothermal imaging mappings of the evaporation system.

Temperature of the system was systematically monitored. Before irradiation, the whole container remained a uniform and low temperature. After irradiation was on, temperature of $BiInSe_3$@NF photothermal converter (bottom of the container) increased first, while that of the upper water remained relatively unchanged. As time went by, high-temperature region gradually spread from $BiInSe_3$@NF photothermal converter to surrounding water and finally throughout the whole container.

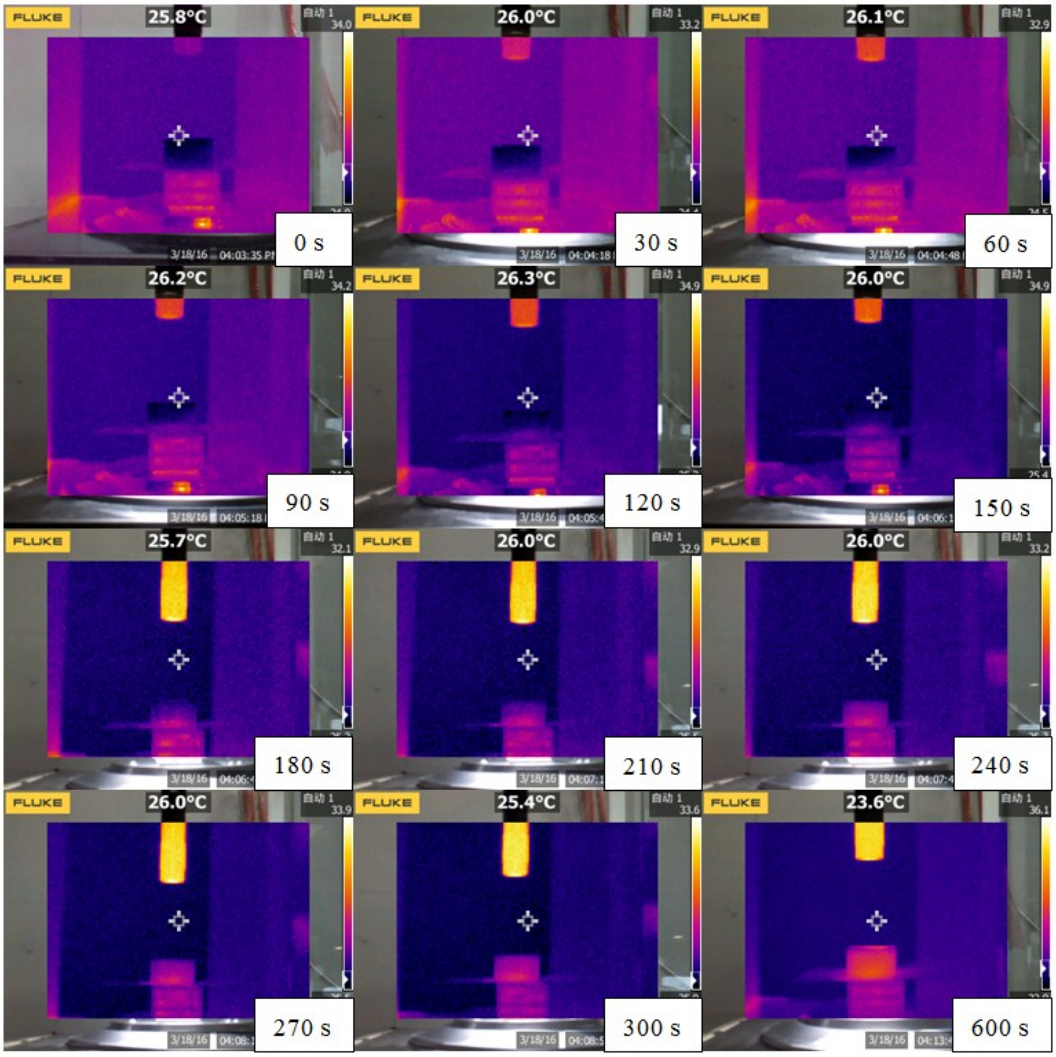

Fig. S6. Photothermal imaging mappings of the evaporation system.

S7. Summary of recent studies on solar energy driven water evaporation.

Table I

Evaporater	E_{Water} (kg m^{-2} h^{-1})	E_{Evap} (kg m^{-2} h^{-1})	E_{Nor}	Ref
$BiInSe_3$@NF	0.33	0.83	2.5	our work
Black TiO_x@SS mesh	0.5195	0.8012	1.54	[1]
Gold-particle-assembly@NPT	0.28	0.63	2.25	[2]
Gold-particle-assembly@NPT	0.38	0.8	2.1	[3]
Black titania	0.56	1.12	2	[4]
Cauliflower-shaped copper nanostructures	ND	ND	2	[5]
Biomimetic nanoparticles	0.44	0.8	1.8	[6]
Carbon-black-based gauze	ND	ND	1.57	[7]
Fe_3O_4/C particles	ND	ND	1.9	[8]

ND: no data.

S8. Absorption coefficient of $BiInSe_3$ over the solar spectrum range.

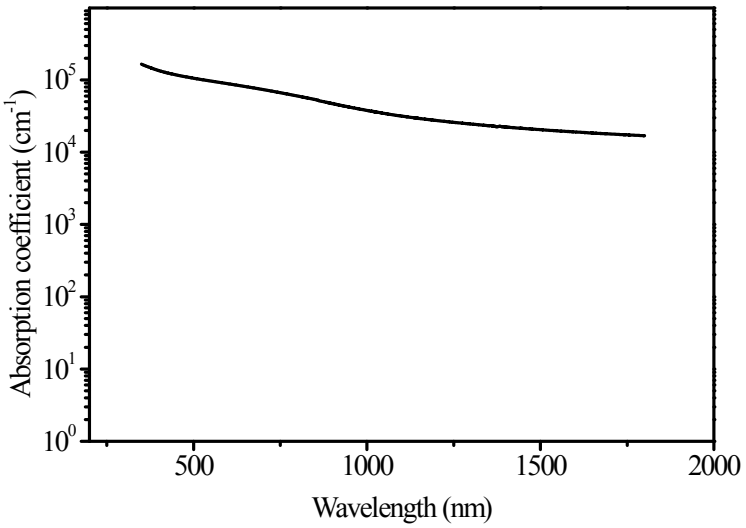

Fig. S7. Absorption coefficient of $BiInSe_3$ over the solar spectrum range.

S9. I-V curves in dark and under illumination of a $BiInSe_3$ photodetector.

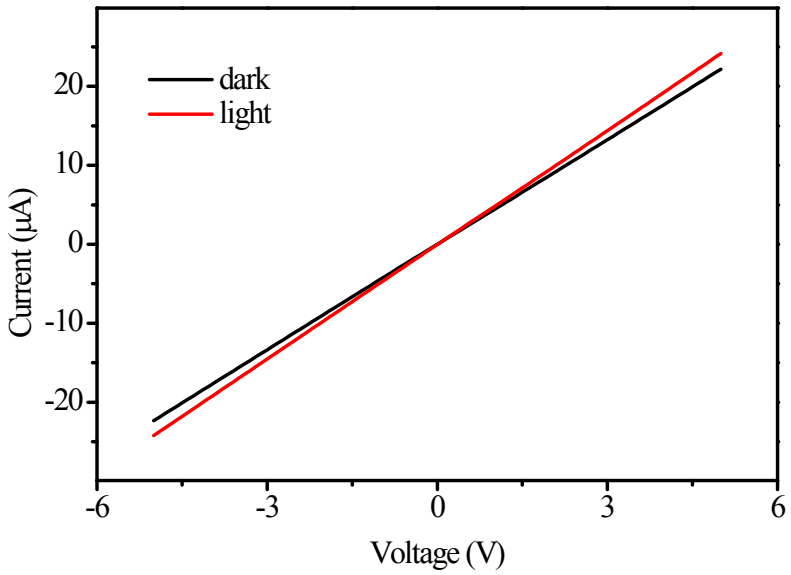

Fig. S8. I-V curves in dark and under illumination of a $BiInSe_3$ photodetector. Wavelength: 635 nm. Power density: 30 mW/cm^2.

References

1 M. Ye, J. Jia, Z. Wu, C. Qian, R. Chen, P. G. O'Brien, W. Sun, Y. Dong and G. A. Ozin, *Adv. Energy Mater.*, 2017, **7**, 201601811.

2 L. Zhou, S. Zhuang, C. He, Y. Tan, Z. Wang and J. Zhu, *Nano Energy*, 2017, **32**, 195-200.

3 L. Zhou, Y. Tan, D. Ji, B. Zhu, P. Zhang, J. Xu, Q. Gan, Z. Yu and J. Zhu, *Sci. Adv.*, 2016, **2**, 1501227.

4 G. Zhu, J. Xu, W. Zhao and F. Huang, *ACS Appl. Mater. Interfaces*, 2016, **8**, 31716-31721.

5 P. Fan, H. Wu, M. Zhong, H. Zhang, B. Bai and G. Jin, *Nanoscale*, 2016, **8**, 14617-14624.

6 C. Liu, J. Huang, C. E. Hsiung, Y. Tian, J. Wang, Y. Han and A. Fratalocchi, *Advanced Sustainable Systems*, 2017, **1**, 1600013.

7 Y. Liu, J. Chen, D. Guo, M. Cao and L. Jiang, *ACS Appl. Mater. Interfaces*, 2015, **7**, 13645-13652.

8 Y. Zeng, J. Yao, B. A. Horri, K. Wang, Y. Wu, D. Li and H. Wang, *Energy Environ. Sci.*, 2011, **4**, 4074-4078.